

Sensitive sensing based on quantum correlation of photons in weak nonlinear regime

Zi-Qiang Yin(尹子强), Zhi-Hao Liu(刘志豪), Jian Tang(唐健), Hui Jing(景辉), and Xun-Wei Xu(徐勋卫)
Citation: Chin. Phys. B, 2026, 35 (**7**): 074201. DOI: 10.1088/1674-1056/ae5c71
http://cpb.iphy.ac.cn; http://iopscience.iop.org/cpb

What follows is a list of articles you may be interested in

In-phase collective unconventional photon blockade and its stability in an asymmetrical cavity containing *N* bosonic atoms

Ying Luo(罗颖), Xinqin Zhang(张新琴), Yi Xiao(肖祎), Jingping Xu(许静平), Haozhen Li(李浩珍), Yaping Yang(羊亚平), and Xiuwen Xia(夏秀文)
Chin. Phys. B, 2025, 34 (**1**): 014203. DOI: 10.1088/1674-1056/ad8cbf

Response analysis of NMRG system considering Rb-Xe coupling

Yi Zhang(张燚), Qiyuan Jiang(江奇渊), Bingfeng Sun(孙兵锋), Jiahu Wei(魏加湖), Lin Yang(杨麟), Yongyuan Li(李永远), Zhiguo Wang(汪之国), Kaiyong Yang(杨开勇), and Hui Luo(罗晖)
Chin. Phys. B, 2024, 33 (**9**): 094203. DOI: 10.1088/1674-1056/ad6130

Quasi-anti-parity—time-symmetric single-resonator micro-optical gyroscope with Kerr nonlinearity

Jingtong Geng(耿靖童), Shuyi Xu(徐书逸), Ting Jin(靳婷), Shulin Ding(丁舒林), Liu Yang(杨柳), Ying Wang(王颖), and Yonggang Zhang(张勇刚)
Chin. Phys. B, 2024, 33 (**1**): 014208. DOI: 10.1088/1674-1056/ad0773

Design and simulation of a silicon-based hybrid integrated optical gyroscope system

Dao-Xin Sun(孙道鑫), Dong-Liang Zhang(张东亮), Li-Dan Lu(鹿利单), Tao Xu(徐涛),Xian-Tong Zheng(郑显通), Zhe-Hai Zhou(周哲海), and Lian-Qing Zhu(祝连庆)
Chin. Phys. B, 2023, 32 (**4**): 044212. DOI: 10.1088/1674-1056/ac81a9

Manipulation of nonreciprocal unconventional photon blockade in a cavity-driven system composed of an asymmetrical cavity and two atoms with weak dipole-dipole interaction

Xinqin Zhang(张新琴), Xiuwen Xia(夏秀文), Jingping Xu(许静平), Haozhen Li(李浩珍), Zeyun Fu(傅泽云), and Yaping Yang(羊亚平)
Chin. Phys. B, 2022, 31 (**7**): 074204. DOI: 10.1088/1674-1056/ac523f

---

RAPID COMMUNICATION

Sensitive sensing based on quantum correlation of photons in weak nonlinear regime

Zi-Qiang Yin(尹子强)[1], Zhi-Hao Liu(刘志豪)[1], Jian Tang(唐健)[1], Hui Jing(景辉)[1,2,3], and Xun-Wei Xu(徐勋卫)[1,2,3,†]

[1] *Key Laboratory of Low-Dimensional Quantum Structures and Quantum Control of Ministry of Education, Key Laboratory for Matter Microstructure and Function of Hunan Province, Department of Physics and Synergetic Innovation Center for Quantum Effects and Applications, Hunan Normal University, Changsha* 410081, *China*

[2] *Hunan Research Center of the Basic Discipline for Quantum Effects and Quantum Technologies, Hunan Normal University, Changsha* 410081, *China*

[3] *Institute of Interdisciplinary Studies, Hunan Normal University, Changsha* 410081, *China*

(Received 18 December 2025; revised manuscript received 25 February 2026; accepted manuscript online 8 April 2026)

Quantum correlation of photons based on quantum interference, such as unconventional photon blockade (UPB), has been extensively studied for realizing single-photon sources in a weak nonlinear regime. However, how to use this effect for other practical applications is rarely studied. Here, we propose to realize angular velocity and temperature sensing based on the quantum correlation of photons induced by quantum interference. We demonstrate that UPB can be observed in the mixing field output from a Mach–Zehnder interferometer (MZI) with two cavities in its two arms based on quantum interference. We show that the second-order correlation function of the output field is sensitive to the parameters of the system, and propose schemes to realize angular velocity and temperature sensing by measuring the second-order correlation of the photons output from the MZI. We find that the second-order correlation function of the output field is much more sensitive to the parameters of the system than the mean photon number, which provides an application scenario for UPB in sensitive sensing.

Keywords: unconventional photon blockade, gyroscope, temperature sensing, Mach–Zehnder interferometer

PACS: 42.50.–p, 42.50.Ar, 42.65.–k

DOI: 10.1088/1674-1056/ae5c71 **CSTR:** 32038.14.CPB.ae5c71

1. Introduction

Quantum correlation of photons can be described by correlation functions,[1,2] which provide a quantitative measure to characterize the quantum nature of light. To date, the application of quantum photon correlation has expanded from characterizing single photons[3,4] to demonstrating photonic quantum logic gates[5,6] and fractional quantum Hall states.[7]

The quantum correlation of photons can be manipulated when they pass through an optical system containing strong photon–photon interaction. If the probabilities of multiphoton states are suppressed by the nonlinear interaction, then the output field becomes sub-Poissonian, which is referred to as conventional photon blockade (CPB).[8] CPB has been proposed in various optical platforms,[9–20] and has been observed in resonators strongly coupled to quantum emitters.[21–27]

In the past decade, some novel mechanisms have been proposed to manipulate the correlation properties of photons under weak nonlinear interactions.[28–40] The one that attracts the most attention is the unconventional photon blockade (UPB),[41,42] where the probabilities of two-photon excitation are suppressed by destructive interference between different transition paths. UPB has been extensively studied in various systems, such as coupled optomechanical systems,[43–45] coupled cavities with second- or third-order nonlinearities,[46–60] a cavity embedded with a two-level atom,[61–66] coupled-resonator chains,[67–69] etc. UPB has been experimentally realized with a quantum dot in a semiconductor cavity quantum electrodynamics system[70] and with a SQUID in superconducting resonators.[71]

In recent work, we found that the photon correlation of the mixing fields output from a Mach–Zehnder interferometer (MZI), with two cavities in the two arms, can be manipulated by quantum interference.[72] We uncover a scaling enhancement of photon blockade in the mixing fields output from the MZI. However, whether strong quantum correlation in the mixing output fields can also be realized in the weak nonlinear regime is still an open question. Moreover, we know that the MZI[73] is a good platform for the measurement of the relative phase acquired by the beam along the two paths, which offers applications in versatile sensing based on the interference pattern.[74–76] How to use the quantum correlation in the mixing fields output from the MZI for sensing is another interesting question.

In this paper, we propose to realize sensitive sensing based on the second-order correlation of mixing fields output from an MZI, with two cavities in the two arms based on weak

†Corresponding author. E-mail: xwxu@hunnu.edu.cn

© 2026 Chinese Physical Society and IOP Publishing Ltd. All rights, including for text and data mining, AI training, and similar technologies, are reserved.

nonlinearity. We find that strong photon blockade can be realized in the weak nonlinear regime by the quantum interference between different paths for two-photon states passing through the MZI. We also show that the second-order correlation of the photons output from the MZI is sensitive to the system parameters, which is the main mechanism for sensing based on quantum correlation.

We note that the angular velocities[77–89] and the temperatures[90–98] are usually measured by monitoring the frequency shift of the system under test. In addition, the Raman-ratio technique based on Stokes/anti-Stokes asymmetry is used to measure temperatures close to absolute zero in the field of cavity optomechanics.[99–104] In contrast, we propose schemes to realize angular velocity sensing and temperature sensing by measuring the second-order correlation of the photons output from the MZI. One of the noteworthy advantages of the sensing scheme based on the second-order correlation is that it can work with a very weak driving field, even at the single-photon level. Moreover, we show that the second-order correlation is much more sensitive to the parameters of the system than the mean photon number, so that the sensing schemes by detecting the second-order correlation may achieve a higher sensitivity than the schemes by measuring the mean photon number.

The remainder of the paper is organized as follows. In Section 2, we present the model of a MZI with two cavities in the two arms. We show UPB in the output field of the MZI both numerically and analytically in Section 3. We demonstrate how to realize versatile sensing by measuring the second-order correlation of the photons output from the MZI in Section 4. Finally, we summarize our main results in Section 5.

2. Physical model

In this paper, we show that UPB based on the quantum interference between different transition paths appears within a narrow range of parameters, and this feature can be applied to realize sensitive sensing. As a specific platform for UPB, we consider an MZI with two cavities (a_1 and a_2) in its two arms, as shown in Fig. 1(a), and discuss the second-order correlation of the output field in the next section. A probe field is divided into two beams by a 50/50 beam splitter (BS), and then injected into one of the cavities, respectively. The transmitted fields from the two cavities are mixed by another 50/50 BS, and a phase shifter (PS) is placed in one of the two arms to change the phase difference between them. The second-order correlation of the output field $a_{\rm out}$ can be measured by a Hanbury–Brown–Twiss (HB-T) set-up. In the frame rotating at the probe laser frequency $\omega_{\rm p}$, the system can be described by the Hamiltonian ($\hbar = 1$)

$$\begin{aligned} H \;=\; & \Delta_1 a_1^\dagger a_1 + U a_1^\dagger a_1^\dagger a_1 a_1 + \Delta_2 a_2^\dagger a_2 \\ & + \mathrm{i}\left(\varepsilon_1 a_1^\dagger + \varepsilon_2 a_2^\dagger - \mathrm{H.c.}\right), \end{aligned} \tag{1}$$

where a_i and $a_i^\dagger$ are the annihilation and creation operators of the cavity mode i with resonance frequency ω_i ($i = 1,2$), $\Delta_i = \omega_i - \omega_{\rm p}$ is the detuning of the probe laser from the cavity resonance, $\delta = \omega_2 - \omega_1$ is the detuning between the two cavity modes, U is the nonlinear interaction strength in cavity mode 1, and $\varepsilon_i = \sqrt{\kappa_i P_{\rm in}/(\hbar\omega_{\rm p})}$ is the driving strength on cavity mode i, with the driving power $P_{\rm in}$ and the decay rate from one of the cavity mirrors κ_i.

The two fields $a_{\rm out}$ and $A_{\rm out}$ output from the MZI can be obtained according to the input–output relation[105]

$$a_{\rm out} = (\sqrt{\kappa_1}a_1 + \mathrm{e}^{\mathrm{i}\phi}\sqrt{\kappa_2}a_2)/\sqrt{2} - a_{\rm vac}, \tag{2}$$

$$A_{\rm out} = (\sqrt{\kappa_1}a_1 - \mathrm{e}^{\mathrm{i}\phi}\sqrt{\kappa_2}a_2)/\sqrt{2} - a'_{\rm vac}, \tag{3}$$

where ϕ is the phase difference between the laser beams output from the two arms (which can be tuned by the PS), and $a_{\rm vac}$, $a'_{\rm vac}$ are the input vacuum fields. As the output field $A_{\rm out}$ can be obtained from $a_{\rm out}$ just by replacing ϕ with $\phi + \pi$, we will only focus on the output field $a_{\rm out}$ in the following.

Here, we focus on the quantum correlation of photons described by the second-order correlation function. The second-order correlation function of the output field $a_{\rm out}$ from the MZI is given by

$$\begin{aligned} g^{(2)}_{\rm out}(\tau) \;\equiv\; & \frac{\left\langle a^\dagger_{\rm out} a^\dagger_{\rm out}(\tau)\, a_{\rm out}(\tau)\, a_{\rm out}\right\rangle}{\left\langle a^\dagger_{\rm out} a_{\rm out}\right\rangle^2} \\ =\; & \sum_{j,k,l,m=1}^{2} \mathrm{e}^{\mathrm{i}n\phi}\sqrt{\kappa_j\kappa_k\kappa_l\kappa_m}\,\frac{\left\langle a_j^\dagger a_k^\dagger(\tau)\, a_l(\tau)\, a_m\right\rangle}{4N^2_{\rm out}}, \end{aligned} \tag{4}$$

where $n = l + m - j - k$, $2N_{\rm out} = \kappa_1\langle a_1^\dagger a_1\rangle + \kappa_2\langle a_2^\dagger a_2\rangle + 2\sqrt{\kappa_1\kappa_2}\mathrm{Re}(\mathrm{e}^{\mathrm{i}\phi}\langle a_1^\dagger a_2\rangle)$, and τ are the time delays between the two photodetectors (D_1 and D_2 in the HB-T set-up). There are cross-correlations between the photons in the two cavities (i.e., $\langle a_2^\dagger a_1^\dagger a_2 a_1\rangle$, $\langle a_1^\dagger a_1^\dagger a_2 a_2\rangle$, $\langle a_1^\dagger a_1^\dagger a_1 a_2\rangle$, and $\langle a_2^\dagger a_1^\dagger a_2 a_2\rangle$), and there are phase factors $\mathrm{e}^{\mathrm{i}n\phi}$ in front of the terms, which can be negative and lead to strong photon blockade in the weak nonlinear regime based on quantum interference.

The system dynamics are governed by the master equation[106] for the density matrix ρ:

$$\frac{\mathrm{d}\rho}{\mathrm{d}t} = -\mathrm{i}\,[H,\rho] + \sum_{i=1,2}\kappa_i\left(2a_i\rho a_i^\dagger - a_i^\dagger a_i\rho - \rho a_i^\dagger a_i\right). \tag{5}$$

In the following discussions, we set $\kappa_1 = \kappa$ as the unit of frequency. We consider a weak nonlinear interaction ($U/\kappa = 0.02$, unless specified otherwise) for two reasons: (i) achieving a strong Kerr nonlinearity in an optical resonator remains a great experimental challenge;[107] (ii) the second-order correlation function of the output field is more sensitive to the system parameters for a weaker nonlinear interaction strength (see Appendix A). To avoid the excitation of multiphoton states, the amplitude of the probe field is also kept weak ($\varepsilon_i/\kappa = 0.1$, unless specified otherwise) to achieve photon blockade.

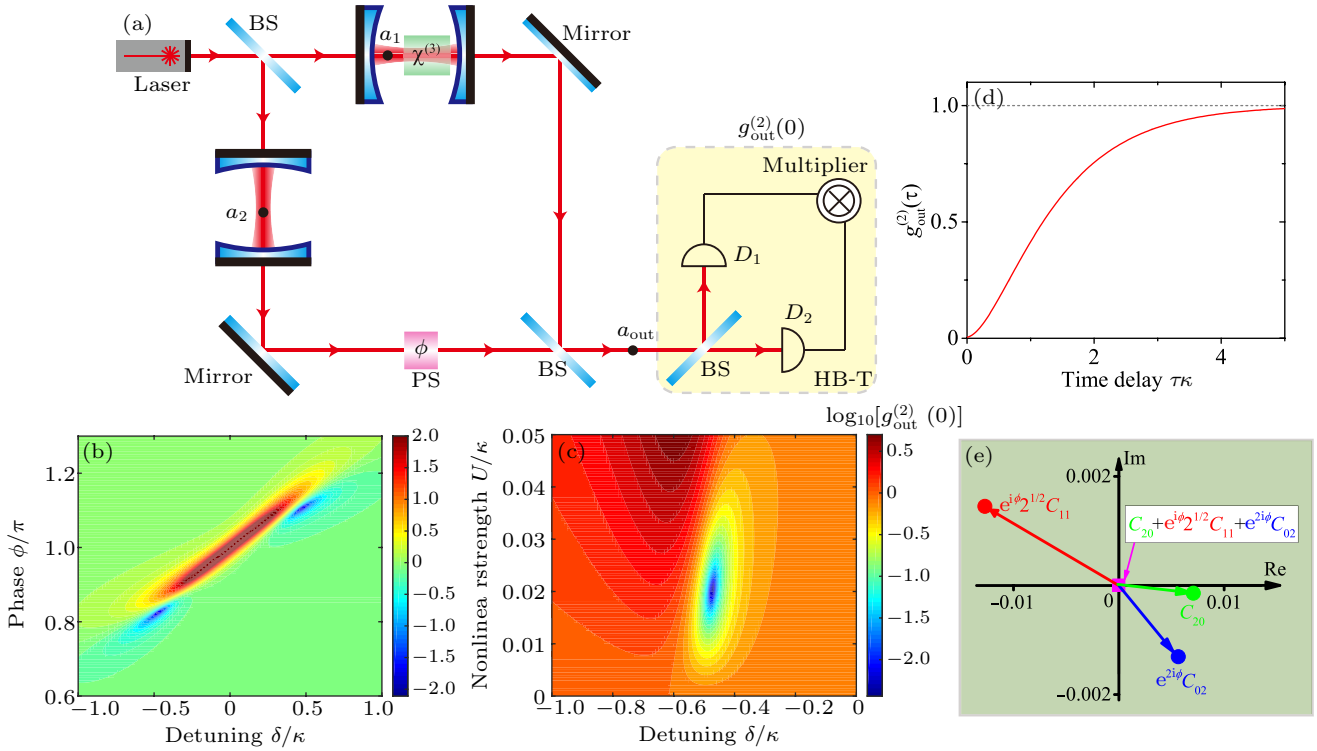


Fig. 1. (a) A Mach–Zehnder interferometer with two cavities (a_1 and a_2) in the two arms. A weak probe field is divided into two beams by a 50/50 beam splitter (BS), and then injected into one of the cavities, respectively. The transmitted fields from these two cavities mix by another 50/50 BS, and a phase shifter (PS) is placed in one of the two arms. The second-order correlation of the output field $a_{\rm out}$ can be measured by a Hanbury–Brown–Twiss (HB-T) set-up. The second-order correlation $\log_{10}[g^{(2)}_{\rm out}(0)]$ (b) versus phase ϕ/π and detuning δ/κ for nonlinear strength $U/\kappa = 0.02$, (c) versus U/κ and detuning δ/κ for $\phi = 0.824\pi$. (d) The second-order correlation $g^{(2)}_{\rm out}(\tau)$ versus time delay $\tau\kappa$, and (e) the probability coefficients of two photons in the cavities (C_{20}, C_{11}, and C_{02}) and in the output field ($C_{20} + e^{i\phi}\sqrt{2}C_{11} + e^{2i\phi}C_{02}$), for $\delta \approx -0.47\kappa$, $\phi = 0.824\pi$, and $U/\kappa = 0.02$. The parameters are $\kappa_1 = \kappa_2 = \kappa$, $\varepsilon_1 = \varepsilon_2 = \kappa/10$, and $\Delta_1 = 0$.

3. Photon blockade with weak nonlinearity

First of all, let us discuss how to realize photon blockade with weak nonlinearity in the MZI. The second-order correlation of the output field $\log_{10}[g^{(2)}_{\rm out}(0)]$ is plotted as a function of the phase ϕ/π and detuning δ/κ for a nonlinear strength of $U/\kappa = 0.02$ in Fig. 1(b) with $\kappa_1 = \kappa_2 = \kappa$. Strong photon anti-bunching $g^{(2)}_{\rm out}(0) \ll 1$ is obtained around the parameters ($\delta \approx -0.47\kappa$, $\phi = 0.824\pi$) and ($\delta \approx 0.47\kappa$, $\phi = 1.104\pi$) with the weak nonlinearity ($U = 0.02\kappa$). In addition, the results for $\kappa_2 \neq \kappa_1$ and different nonlinear strengths U are shown in the Appendix, which show two points: (i) $\kappa_2 \neq \kappa_1$ mainly shifts the optimal detuning δ for photon blockade; (ii) $g^{(2)}_{\rm out}(0) < 1$ appears in a narrower parameter range for a weaker nonlinear interaction strength.

The second-order correlation $\log_{10}[g^{(2)}_{\rm out}(0)]$ is also plotted as a function of the nonlinear interaction strength U/κ and detuning δ/κ for $\phi = 0.824\pi$ in Fig. 1(c). The minimal value of $\log_{10}[g^{(2)}_{\rm out}(0)]$ is obtained around $U = 0.02\kappa$. The second-order correlation $g^{(2)}_{\rm out}(\tau)$ versus time delay $\tau\kappa$ is shown in Fig. 1(d). Different from the rapid oscillations induced by the coupling between two cavities predicted in weakly nonlinear photonic molecules, [41,42] here there is no oscillation behavior as the delay time goes on, and the scale of the time delay is determined by the decay rate of the cavities as $1/\kappa$.

In order to understand the origin of the strong antibunching, we consider a non-Hermitian Hamiltonian including the decay effect as $H' = H - i\kappa_1 a_1^\dagger a_1 - i\kappa_2 a_2^\dagger a_2$ and use the wave function terminated to the two-photon states as

$$\begin{aligned}|\psi\rangle \;=\; & C_{00}|0,0\rangle + C_{10}|1,0\rangle + C_{01}|0,1\rangle \\ & + C_{20}|2,0\rangle + C_{11}|1,1\rangle + C_{02}|0,2\rangle, \end{aligned} \tag{6}$$

for weak probe fields $\varepsilon_i \ll \{\kappa_1, \kappa_2\}$. Substituting the non-Hermitian Hamiltonian and wave function into the Schrödinger's equation $i\hbar\frac{\partial}{\partial t}|\psi\rangle = H'|\psi\rangle$, we get the dynamical equations for the probability coefficients as

$$i\frac{\mathrm{d}}{\mathrm{d}t}C_{10} = (\Delta_1 - i\kappa_1)C_{10} + i\varepsilon_1 C_{00}, \tag{7}$$

$$i\frac{\mathrm{d}}{\mathrm{d}t}C_{01} = (\Delta_2 - i\kappa_2)C_{01} + i\varepsilon_2 C_{00}, \tag{8}$$

$$i\frac{\mathrm{d}}{\mathrm{d}t}C_{20} = (2\Delta_1 + 2U - i2\kappa_1)C_{20} + i\sqrt{2}\varepsilon_1 C_{10}, \tag{9}$$

$$i\frac{\mathrm{d}}{\mathrm{d}t}C_{02} = (2\Delta_2 - i2\kappa_2)C_{02} + i\sqrt{2}\varepsilon_2 C_{01}, \tag{10}$$

$$i\frac{\mathrm{d}}{\mathrm{d}t}C_{11} = (\Delta_1 + \Delta_2 - i\kappa_1 - i\kappa_2)C_{11} + i\varepsilon_2 C_{10} + i\varepsilon_1 C_{01}. \tag{11}$$

In the steady state, i.e., $\mathrm{d}C_{ij}/\mathrm{d}t = 0$, the linear equations for the probability coefficients are given by

$$0 = (\Delta_1 - i\kappa_1)C_{10} + i\varepsilon_1 C_{00}, \tag{12}$$

$$0 = (\Delta_2 - \mathrm{i}\kappa_2)C_{01} + \mathrm{i}\varepsilon_2 C_{00}, \tag{13}$$

$$0 = (2\Delta_1 + 2U - \mathrm{i}2\kappa_1)C_{20} + \mathrm{i}\sqrt{2}\varepsilon_1 C_{10}, \tag{14}$$

$$0 = (2\Delta_2 - \mathrm{i}2\kappa_2)C_{02} + \mathrm{i}\sqrt{2}\varepsilon_2 C_{01}, \tag{15}$$

$$0 = (\Delta_1 + \Delta_2 - \mathrm{i}\kappa_1 - \mathrm{i}\kappa_2)C_{11} + \mathrm{i}\varepsilon_2 C_{10} + \mathrm{i}\varepsilon_1 C_{01}. \tag{16}$$

Under the weak driving conditions ($\varepsilon_i \ll \{\kappa_1, \kappa_2\}$), we have $C_{00} \approx 1 \gg \{|C_{10}|, |C_{01}|\} \gg \{|C_{20}|, |C_{02}|, |C_{11}|\}$. By setting $\Delta_1 = 0$ and $\varepsilon_1 = \varepsilon$, we have $\Delta_2 = \delta$ and $\varepsilon_2 = \varepsilon\sqrt{\kappa_2/\kappa_1}$ for the same driving power on the two cavities. Thus, the expressions of the probability coefficients are given by

$$C_{10} = \frac{\varepsilon}{\kappa_1}, \tag{17}$$

$$C_{01} = \frac{-\mathrm{i}\varepsilon}{\delta - \mathrm{i}\kappa_2}\sqrt{\frac{\kappa_2}{\kappa_1}} \tag{18}$$

for single-photon states, and by

$$C_{20} = \frac{-\mathrm{i}}{U - \mathrm{i}\kappa_1}\frac{\varepsilon^2}{\sqrt{2}\kappa_1}, \tag{19}$$

$$C_{02} = -\frac{1}{\sqrt{2}}\frac{\kappa_2}{\kappa_1}\frac{\varepsilon^2}{(\delta - \mathrm{i}\kappa_2)^2}, \tag{20}$$

$$C_{11} = -\frac{\mathrm{i}\varepsilon^2}{\kappa_1(\delta - \mathrm{i}\kappa_2)}\sqrt{\frac{\kappa_2}{\kappa_1}} \tag{21}$$

for two-photon states.

Based on the probability coefficients, the output photon intensity N_{out}/κ and second-order correlation function $g^{(2)}_{\mathrm{out}}(0)$ can be expressed as

$$N_{\mathrm{out}} \approx \frac{1}{2}\left|\sqrt{\kappa_1}C_{10} + \sqrt{\kappa_2}\,\mathrm{e}^{\mathrm{i}\phi}C_{01}\right|^2, \tag{22}$$

$$g^{(2)}_{\mathrm{out}}(0) \approx \frac{2\left|\kappa_1 C_{20} + \sqrt{2\kappa_1\kappa_2}\,\mathrm{e}^{\mathrm{i}\phi}C_{11} + \kappa_2\,\mathrm{e}^{\mathrm{i}2\phi}C_{02}\right|^2}{\left|\sqrt{\kappa_1}C_{10} + \sqrt{\kappa_2}\,\mathrm{e}^{\mathrm{i}\phi}C_{01}\right|^4}. \tag{23}$$

The optimal conditions for photon blockade are obtained from

$$\kappa_1 C_{20} + \sqrt{2\kappa_1\kappa_2}\,\mathrm{e}^{\mathrm{i}\phi}C_{11} + \kappa_2\,\mathrm{e}^{\mathrm{i}2\phi}C_{02} = 0, \tag{24}$$

and they are given by

$$\frac{\delta_{\mathrm{opt}}}{\kappa_2} \approx \pm\sqrt{\frac{\sqrt{2U/\kappa_1} - U/\kappa_1}{1 - \sqrt{2U/\kappa_1} + U/\kappa_1}}, \tag{25}$$

$$\phi_{\mathrm{opt}} = \arg\left[-\left(1 + \mathrm{i}\frac{\delta_{\mathrm{opt}}}{\kappa_2}\right)\left(1 - \mathrm{e}^{\mathrm{i}\frac{\pi}{4}}\sqrt{\frac{U}{\kappa_1}}\right)\right], \tag{26}$$

for the weak nonlinearity $U \ll \kappa_1$.

To understand the conditions for photon blockade intuitively, the probability coefficients of two photons in the cavities (C_{20}, C_{11}, and C_{02}) and in the output field ($C_{20} + \mathrm{e}^{\mathrm{i}\phi}\sqrt{2}C_{11} + \mathrm{e}^{2\mathrm{i}\phi}C_{02}$) are shown in Fig 1(e), with the parameters ($\kappa_1 = \kappa_2 = \kappa$, $\delta \approx -0.47\kappa$, $\phi = 0.824\pi$, $U/\kappa = 0.02$) for minimal of $g^{(0)}_{\mathrm{out}}$. In addition, when $\kappa_1 \neq \kappa_2$ (see Appendix A), we find that δ_{opt} linearly depends on the decay rate κ_2 of cavity mode 2, but ϕ_{opt} is independent of κ_2, which agree well with Eqs. (24)–(26).

4. Quantum sensing based on photon blockade

We know that both the output photon intensity N_{out}/κ and the second-order correlation function $g^{(2)}_{\mathrm{out}}(0)$ depend on system parameters such as the phase ϕ and the detuning δ, as shown in Fig. 2. From the figure, we can see that the phase interval $\Delta\phi$ of the second-order correlation function from its minimum value $g^{(2)}_{\mathrm{out}}(0) = 0.0044$ (antibunching) to its maximum value $g^{(2)}_{\mathrm{out}}(0) = 7.15$ (bunching) is about $\Delta\phi \approx \pi/20$, which is much narrower than the phase interval ($\Delta\phi \approx \pi$) from the maximum to minimum value of the output photon intensity N_{out}/κ. The frequency interval $\Delta\omega$ between the maximum value $g^{(2)}_{\mathrm{out}}(0) = 1.91$ (bunching) and the minimum value $g^{(2)}_{\mathrm{out}}(0) = 0.0044$ (antibunching) is about $\Delta\omega \approx 0.18\kappa$, which is also much narrower than the frequency interval ($\Delta\omega \approx 2.4\kappa$) from the maximum to minimum value of N_{out}/κ. That is, the second-order correlation function $g^{(2)}_{\mathrm{out}}(0)$ is much more sensitive to the parameters than the output photon intensity N_{out}/κ. This interesting effect can be understood by the fact that under the weak driving condition, the change of $g^{(2)}_{\mathrm{out}}(0)$ mainly originates from destructive interference among the three paths for two photons passing through the system [see Eq. (23)]; while the output photon intensity N_{out}/κ depends on the interference between the two paths for one photon passing through the system [see Eq. (22)]; in special parameter region, the interference among the three paths for two photons is much more sensitive to the parameters than the interference between the two paths for one photon. Such effect provides us the key mechanism for sensitive sensing based on the second-order correlation. As examples, here we will propose two schemes to realize angular velocity sensing and temperature sensing, respectively, by measuring the second-order correlation of the photons output from the MZI.

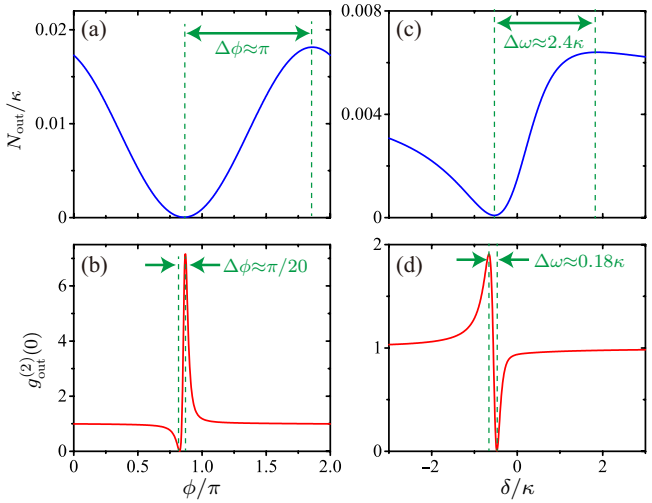


Fig. 2. The output photon intensity N_{out}/κ and second-order correlation function $g^{(2)}_{\mathrm{out}}(0)$, (a), (b) versus phase ϕ/π with detuning $\delta/\kappa \approx -0.47$, and (c), (d) versus δ/κ with $\phi = 0.824\pi$. The other parameters are the same as those in Fig. 1(d).

4.1. Angular velocity sensing (gyroscope)

As a specific example, we consider the case in which the platform rotates with an angular velocity Ω as shown in Fig. 3(a), which leads to an additional phase difference $\Delta\phi$ between the two beams as

$$\Delta\phi = \frac{4\pi A}{\lambda_0 c}\Omega, \tag{27}$$

where A is the area enclosed by the optical paths, λ_0 is the wavelength of the incident light, and c is the speed of light in vacuum. We set the phase difference $\phi_0 = 0.85\pi$ for the platform to zero in the steady state, so we have the total phase difference $\phi = 0.85\pi + \Delta\phi$ for the system rotating with an angular velocity Ω. In the following numerical calculations, we take the parameters:[108] incident light with a wavelength of $\lambda_0 = 1550$ nm, and two fiber coils with the same length $L = 5$ km and diameter $D = 40$ cm, i.e., the total effective area is $A = (2 \times L \times D)/4 = 10^3$ m^2. The two optical cavities are formed between the two fiber-mirrors.[109]

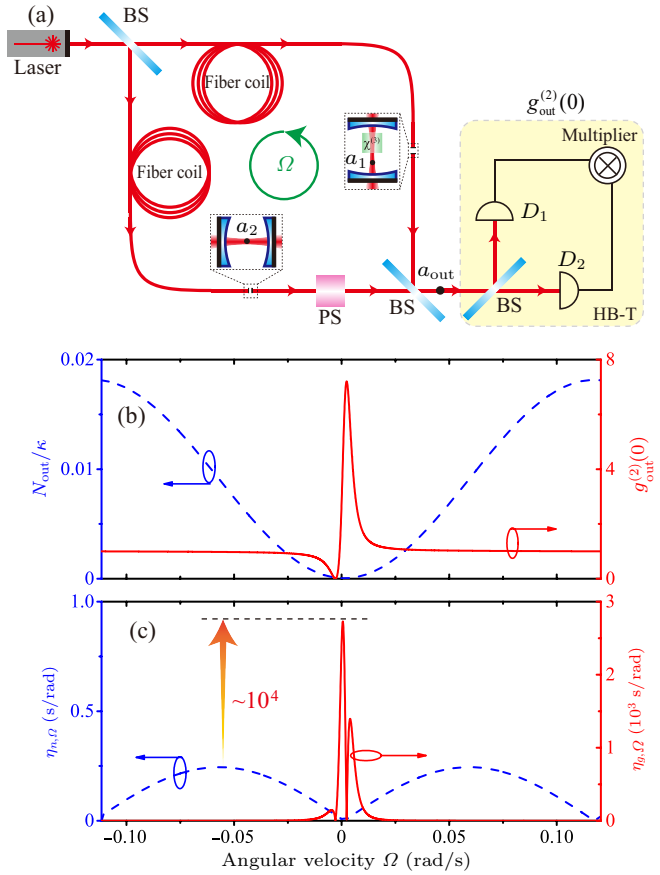


Fig. 3. (a) The scheme to sense the angular frequency Ω by measuring the second-order correlation function $g^{(2)}_{\rm out}(0)$ of the output photons. (b) The output photon intensity $N_{\rm out}/\kappa$ and second-order correlation function $g^{(2)}_{\rm out}(0)$ versus Ω. (c) The sensitivities $\eta_{n,\Omega}$ and $\eta_{g,\Omega}$ versus Ω. The parameters are the same as those in Fig. 1(d).

The output photon intensity $N_{\rm out}/\kappa$ and second-order correlation function $g^{(2)}_{\rm out}(0)$ are plotted as functions of the angular velocity Ω in Fig. 3(b). We can see that the second-order correlation function $g^{(2)}_{\rm out}(0)$ is much more sensitive to changes in the angular velocity Ω than the photon intensity $N_{\rm out}/\kappa$. To characterize the sensitivity of $N_{\rm out}/\kappa$ and $g^{(2)}_{\rm out}(0)$ to changes in the angular velocity Ω, we can define the sensitivity coefficients as

$$\eta_{n,\Omega} = \frac{{\rm d}N_{\rm out}/\kappa}{{\rm d}\Omega}, \tag{28}$$

$$\eta_{g,\Omega} = \frac{{\rm d}g^{(2)}_{\rm out}(0)}{{\rm d}\Omega}. \tag{29}$$

The sensitivities $\eta_{n,\Omega}$ and $\eta_{g,\Omega}$ are plotted as functions of the angular velocity Ω in Fig. 3(c). The maximal value of $\eta_{g,\Omega}$ is about four orders of magnitude greater than that of $\eta_{n,\Omega}$. It is known that the rotational angular velocity of the Earth is about $\Omega_{\rm earth} = 7.3 \times 10^{-5}$ rad/s, and we have $g^{(2)}_{\rm out}(0) = 2.79$ for $\Omega = 0$ and $g^{(2)}_{\rm out}(0) = 2.97$ for $\Omega = \Omega_{\rm earth}$. We note that the detection of the second-order correlation of photons has been widely used to test the performance of single-photon sources,[110] and the standard deviation of the second-order correlation function smaller than 0.01 is within the reach of current technology.[111–113] Thus we can detect the rotation of the Earth by measuring the second-order correlation function $g^{(2)}_{\rm out}(0)$ of the photons output from the MZI.

4.2. Temperature sensing

In this subsection, we consider a dielectric layer in the cavity a_2 as shown in Fig. 4(a), and discuss how to measure the change in temperature based on the thermal effect. Such a setup can be realized with a dielectric membrane placed between two macroscopic, rigid, high-finesse mirrors, which has been widely used to investigate the coupling between macroscopic mechanical resonators and the electromagnetic field through radiation pressure, also known as the "membrane-in-the-middle" optomechanical system.[114–117] Moreover, the Fabry–Pérot (FP) cavity can also be formed between the ends of two single-mode optical fibers with smooth concave depressions machined using a laser ablation technique, and the dielectric membrane can be held in a fixed mount attached to a piezoelectric scanner, providing linear motion along the axis of the FP cavity.[118–120] Due to thermal expansion, the thickness of the dielectric layer changes as

$$d(T) = d_0\,(1 + \alpha\Delta T)\,, \tag{30}$$

where d_0 is the thickness of the dielectric layer at a reference temperature, α is the thermal expansion coefficient, and ΔT is the temperature variation. In addition, because of the thermal-optical effect, the refractive index also depends on the temperature as

$$n(T) = n_0\,(1 + \beta\Delta T)\,, \tag{31}$$

where n_0 is the refractive index at a reference temperature and β is the thermal-optic coefficient. Based on these two factors,

the frequency shift of the cavity a_2 is given approximately as

$$\delta_{\rm th} \approx -\omega_2 \left[\frac{n_0 d_0}{L}\beta + \frac{(n_0-1)\,d_0}{L}\alpha\right]\Delta T, \tag{32}$$

where ω_2 is the eigenfrequency of the cavity a_2 at a reference temperature with a cavity length L. Under the condition that $\omega_2 - \omega_1 = -0.56\kappa$, we have the detuning $\delta = -0.56\kappa + \delta_{\rm th}$. As a simple example, we consider the dielectric layer as a SiO_2 layer, with the typical parameters:[121,122] $\alpha = 5.5\times10^{-7}\ ^\circ{\rm C}^{-1}$, and $\beta = 1.0\times10^{-5}\ ^\circ{\rm C}^{-1}$, $n_0 = 1.45$ at the reference temperature 25 °C, $\lambda_0 = 1550$ nm, $\omega_2 = 2\pi c/\lambda_0$, and $\omega_2/\kappa = 10^7$. The other parameters are $d_0 = 0.01$ mm and $L = 1$ mm.

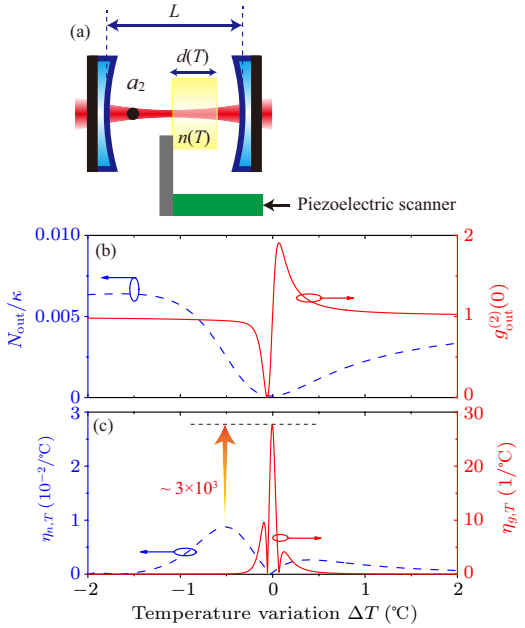


Fig. 4. (a) The part of cavity mode 2 for the temperature measurement, and all other parts are the same as those in Fig. 1(a). (b) The output photon intensity $N_{\rm out}/\kappa$ and second-order correlation function $g^{(2)}_{\rm out}(0)$ versus ΔT. (c) The sensitivities $\eta_{n,T}$ and $\eta_{g,T}$ versus ΔT. The parameters are the same as those in Fig. 1(d).

The output photon intensity $N_{\rm out}/\kappa$ and second-order correlation function $g^{(2)}_{\rm out}(0)$ are plotted as functions of temperature variation ΔT in Fig. 4(b). We can see that the second-order correlation function $g^{(2)}_{\rm out}(0)$ is much more sensitive to the variation of the temperature ΔT than the output photon intensity $N_{\rm out}/\kappa$. To characterize the sensitivity of $N_{\rm out}/\kappa$ and $g^{(2)}_{\rm out}(0)$ with respect to ΔT, we can define the sensitivity coefficients as

$$\eta_{n,T} = \frac{{\rm d}N_{\rm out}/\kappa}{{\rm d}T}, \tag{33}$$

$$\eta_{g,T} = \frac{{\rm d}g^{(2)}_{\rm out}(0)}{{\rm d}T}. \tag{34}$$

The sensitivities $\eta_{n,T}$ and $\eta_{g,T}$ are plotted as functions of the temperature variation ΔT in Fig. 4(c). The maximal value of $\eta_{g,T}$ is about 28 $^\circ{\rm C}^{-1}$, which is 3×10^3 times greater than the maximal value of $\eta_{n,T}$.

5. Conclusions

In this paper, we propose schemes to achieve sensitive sensing based on the UPB appearing in a narrow range of parameters. We demonstrate that UPB can be achieved in the mixed-field output from the two cavities, in the two arms of an MZI, even in the weak nonlinear regime. Based on the UPB, we propose schemes to realize angular velocity and temperature sensing by measuring the second-order correlation of the photons output from the MZI, and show that the second-order correlation of the photons is much more sensitive to the system parameters than the mean photon number. On the one hand, our work provides a new perspective for using UPB in practical sensing applications; on the other hand, we propose a possible strategy to realize sensitive sensing based on the quantum correlation properties of an optical field with a very weak driving strength. In this strategy, the measurement processes are realized by using single-photon detectors, rather than a spectrometer, which at least provides a supplementary solution to traditional sensing schemes. Finally, a number of potential limitations of the sensing schemes based on the second-order correlation need to be considered. First, the sensing region through the second-order correlation is much narrower than that of the photon intensity. Second, the angular velocity and temperature resolution is limited by the measuring instruments of the second-order correlation. These limitations, however, point to the following directions for future research.

Appendix A: Numerical results for different U and κ_2

Here, we will investigate the effect of the nonlinear strength U and the difference between κ_2 and κ_1 on the second-order correlation. $\log_{10}[g^{(2)}_{\rm out}(0)]$ versus phase ϕ/π and detuning δ/κ for different U are shown in Figs. A1(a) and A1(b). Through comparison of the results for different U, i.e., Figs. 1(b), A1(a), and A1(b), we find that, besides the optimal detuning δ/κ and phase ϕ/π for photon blockade being different, $g^{(2)}_{\rm out}(0) < 1$ can be achieved in a wider region by a larger nonlinear strength, which is positive for realizing single-photon sources. However, $g^{(2)}_{\rm out}(0)$ is more sensitive to the parameters of the system for a weaker nonlinear interaction strength, which is more suitable for sensitive sensing.

The second-order correlation $\log_{10}[g^{(2)}_{\rm out}(0)]$ for $\kappa_2 \neq \kappa_1 = \kappa$ is shown in Figs. A1(c) and A1(d). Specifically, the optimal detuning for photon blockade is $\delta/\kappa = -0.42$ for $\kappa_2 = 0.9\kappa_1$ [Fig. A1(c)], $\delta/\kappa = -0.47$ for $\kappa_2 = \kappa_1$ [Fig. A1(b)], and $\delta/\kappa = -0.52$ for $\kappa_2 = 1.1\kappa_1$ [Fig. A1(d)], which show that the optimal detuning for photon blockade linearly depends on the decay rate κ_2. In contrast, the optimal phase for photon blockade is the same ($\phi/\pi = 0.824$) for different κ_2. These numerical results agree well with Eqs. (24)–(26). Moreover,

there is no significant difference in the parameter range for $g^{(2)}_{\rm out}(0) < 1$ with $|\kappa_1 - \kappa_2| < 0.1\kappa_1$, which means that the main conclusions in the main text still work when a slight difference is present between the two decay rates.

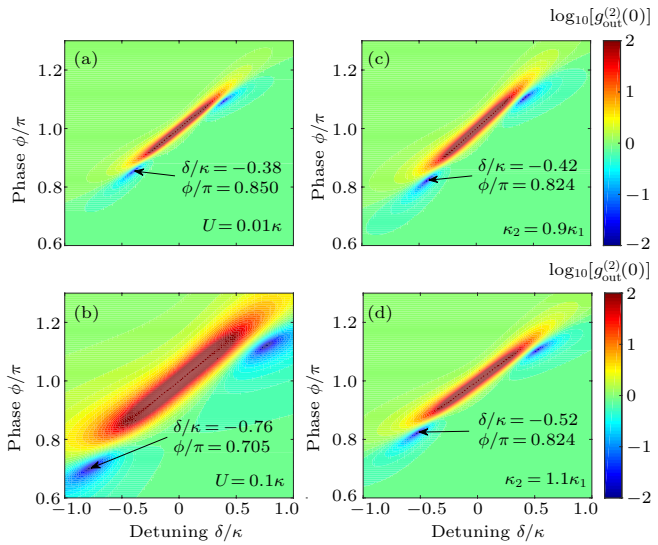


Fig. A1. The second-order correlation $\log_{10}[g^{(2)}_{\rm out}(0)]$ versus phase ϕ/π and detuning δ/κ for (a) $U = 0.01\kappa$, $\kappa_1 = \kappa_2$; (b) $U = 0.1\kappa$, $\kappa_1 = \kappa_2$; (c) $U = 0.02\kappa$, $\kappa_2 = 0.9\kappa_1$; (d) $U = 0.02\kappa$, $\kappa_2 = 1.1\kappa_1$. The other parameters are the same as those in Fig. 1(b).

Acknowledgements

This work is supported by Quantum Science and Technology – National Science and Technology Major Project of China (Grant No. 2024ZD0301000), the National Natural Science Foundation of China (Grant Nos. 12064010, 12247105, 11935006, and 12421005), the National Key R&D Program of China (Grant No. 2024YFE0102400), and Hunan Provincial Major Sci-Tech Program (Grant No. 2023ZJ1010).

References

[1] Glauber R J 1963 *Phys. Rev. Lett.* **10** 84
[2] Glauber R J 1963 *Phys. Rev.* **130** 2529
[3] Buckley S, Rivoire K and Vučković J 2012 *Rep. Prog. Phys.* **75** 126503
[4] Lodahl P, Mahmoodian S and Stobbe S 2015 *Rev. Mod. Phys.* **87** 347
[5] Shi S, Xu B, Zhang K, Ye G S, Xiang D S, Liu Y, Wang J, Su D and Li L 2022 *Nat. Commun.* **13** 4454
[6] Li M, Zhang Y L, Tang H X, Dong C H, Guo G C and Zou C L 2020 *Phys. Rev. Appl.* **13** 044013
[7] Wang C, Liu F M, Chen M C, Chen H, Zhao X H, Ying C, Shang Z X, Wang J W, Huo Y H, Peng C Z, Zhu X, Lu C Y and Pan J W 2024 *Science* **384** 579
[8] Imamoğlu A, Schmidt H, Woods G and Deutsch M 1997 *Phys. Rev. Lett.* **79** 1467
[9] Ridolfo A, Leib M, Savasta S and Hartmann M J 2012 *Phys. Rev. Lett.* **109** 193602
[10] Liu Y X, Xu X W, Miranowicz A and Nori F 2014 *Phys. Rev. A* **89** 043818
[11] Miranowicz A, Bajer J, Paprzycka M, Liu Y X, Zagoskin A M and Nori F 2014 *Phys. Rev. A* **90** 033831
[12] Rabl P 2011 *Phys. Rev. Lett.* **107** 063601
[13] Nunnenkamp A, Børkje K and Girvin S M 2011 *Phys. Rev. Lett.* **107** 063602
[14] Liao J Q and Nori F 2013 *Phys. Rev. A* **88** 023853
[15] Xie H, Lin G W, Chen X, Chen Z H and Lin X M 2016 *Phys. Rev. A* **93** 063860
[16] Majumdar A and Gerace D 2013 *Phys. Rev. B* **87** 235319
[17] Huang R, Miranowicz A, Liao J Q, Nori F and Jing H 2018 *Phys. Rev. Lett.* **121** 153601
[18] Huang R, Özdemir Ş K, Liao J Q, Minganti F, Kuang L M, Nori F and Jing H 2022 *Laser Photon. Rev.* **16** 2100430
[19] Chakram S, He K, Dixit A V, Oriani A E, Naik R K, Leung N, Kwon H, Ma W L, Jiang L and Schuster D I 2022 *Nat. Phys.* **18** 879
[20] Zhou Y H, Zhang X Y, Wu Q C, Ye B L, Zhang Z Q, Zou D D, Shen H Z and Yang C P 2020 *Phys. Rev. A* **102** 033713
[21] Birnbaum K M, Boca A, Miller R, Boozer A D, Northup T E and Kimble H J 2005 *Nature* **436** 87
[22] Dayan B, Parkins A S, Aoki T, Ostby E P, Vahala K J and Kimble H J 2008 *Science* **319** 1062
[23] Aoki T, Parkins A S, Alton D J, Regal C A, Dayan B, Ostby E, Vahala K J and Kimble H J 2009 *Phys. Rev. Lett.* **102** 083601
[24] Faraon A, Fushman I, Englund D, Stoltz N, Petroff P and Vučković J 2008 *Nat. Phys.* **4** 859
[25] Reinhard A, Volz T, Winger M, Badolato A, Hennessy K J, Hu E L and Imamoğlu A 2012 *Nature Photon.* **6** 93
[26] Lang C, Bozyigit D, Eichler C, Steffen L, Fink J M, Abdumalikov A A, Baur M, Filipp S, da Silva M P, Blais A and Wallraff A 2011 *Phys. Rev. Lett.* **106** 243601
[27] Hoffman A J, Srinivasan S J, Schmidt S, Spietz L, Aumentado J, Türeci H E and Houck A A 2011 *Phys. Rev. Lett.* **107** 053602
[28] Lingenfelter A, Roberts D and Clerk A A 2021 *Sci. Adv.* **7** eabj1916
[29] Ma Y X and Li P B 2023 *Phys. Rev. A* **108** 053709
[30] Zhou Y H, Zhang X Y, Liu T, Wu Q C, Shi Z C, Shen H Z and Yang C P 2022 *Phys. Rev. Appl.* **18** 064009
[31] Su X, Tang J S and Xia K 2022 *Phys. Rev. A* **106** 063707
[32] Ben-Asher A, Fernández-Domínguez A I and Feist J 2023 *Phys. Rev. Lett.* **130** 243601
[33] Zuo Y, Huang R, Kuang L M, Xu X W and Jing H 2022 *Phys. Rev. A* **106** 043715
[34] Kryuchkyan G Y, Shahinyan A R and Shelykh I A 2016 *Phys. Rev. A* **93** 043857
[35] Hovsepyan G H, Shahinyan A R and Kryuchkyan G Y 2014 *Phys. Rev. A* **90** 013839
[36] Kyriienko O and Liew T C H 2014 *Phys. Rev. A* **90** 063805
[37] Ghosh S and Liew T C H 2018 *Phys. Rev. B* **97** 241301
[38] Ghosh S and Liew T C H 2019 *Phys. Rev. Lett.* **123** 013602
[39] Li M, Zhang Y L, Wu S H, Dong C H, Zou X B, Guo G C and Zou C L 2022 *Phys. Rev. Lett.* **129** 043601
[40] Stefanatos D and Paspalakis E 2020 *Phys. Rev. A* **102** 013716
[41] Liew T C H and Savona V 2010 *Phys. Rev. Lett.* **104** 183601
[42] Bamba M, Imamoğlu A, Carusotto I and Ciuti C 2011 *Phys. Rev. A* **83** 021802
[43] Xu X W and Li Y J 2013 *J. Phys. B: At. Mol. Opt. Phys.* **46** 035502
[44] Savona V 2013 arXiv: 1302.5937
[45] Zhang W Z, Cheng J, Liu J Y and Zhou L 2015 *Phys. Rev. A* **91** 063836
[46] Ferretti S, Savona V and Gerace D 2013 *New J. Phys.* **15** 025012
[47] Flayac H and Savona V 2013 *Phys. Rev. A* **88** 033836
[48] Gerace D and Savona V 2014 *Phys. Rev. A* **89** 031803
[49] Xu X W and Li Y 2014 *Phys. Rev. A* **90** 043822
[50] Xu X W and Li Y 2014 *Phys. Rev. A* **90** 033809
[51] Lemonde M A, Didier N and Clerk A A 2014 *Phys. Rev. A* **90** 063824
[52] Shen H Z, Zhou Y H and Yi X X 2015 *Phys. Rev. A* **91** 063808
[53] Zhou Y H, Shen H Z and Yi X X 2015 *Phys. Rev. A* **92** 023838
[54] Flayac H and Savona V 2017 *Phys. Rev. A* **96** 053810
[55] Sarma B and Sarma A K 2017 *Phys. Rev. A* **96** 053827
[56] Zhou Y H, Minganti F, Qin W, Wu Q C, Zhao J L, Fang Y L, Nori F and Yang C P 2021 *Phys. Rev. A* **104** 053718
[57] Shen S, Qu Y, Li J and Wu Y 2019 *Phys. Rev. A* **100** 023814
[58] Zubizarreta Casalengua E, López Carreño J C, Laussy F P and del Valle E 2020 *Laser Photon. Rev.* **14** 1900279
[59] Zubizarreta Casalengua E, López Carreño J C, Laussy F P and del Valle E 2020 *Phys. Rev. A* **101** 063824
[60] Wang D Y, Bai C H, Liu S, Zhang S and Wang H F 2020 *New J. Phys.* **22** 093006
[61] Majumdar A, Bajcsy M, Rundquist A and Vučković J 2012 *Phys. Rev. Lett.* **108** 183601
[62] Zhang W, Yu Z, Liu Y and Peng Y 2014 *Phys. Rev. A* **89** 043832
[63] Tang J, Geng W and Xu X 2015 *Sci. Rep.* **5** 9252

[64] Liang X, Duan Z, Guo Q, Liu C, Guan S and Ren Y 2019 *Phys. Rev. A* **100** 063834
[65] Kyriienko O, Krizhanovskii D N and Shelykh I A 2020 *Phys. Rev. Lett.* **125** 197402
[66] Liu X, Tian M Y, Cui X N and Zhang X H 2024 *Chin. Phys. B* **33** 020308
[67] Wang Y, Verstraelen W, Zhang B, Liew T C H and Chong Y D 2021 *Phys. Rev. Lett.* **127** 240402
[68] Li J, Hu C M and Yang Y 2024 *Phys. Rev. Appl.* **21** 034058
[69] Lu Z G, Wu Y and Lü X Y 2025 *Phys. Rev. Lett.* **134** 013602
[70] Snijders H J, Frey J A, Norman J, Flayac H, Savona V, Gossard A C, Bowers J E, van Exter M P, Bouwmeester D and Löffler W 2018 *Phys. Rev. Lett.* **121** 043601
[71] Vaneph C, Morvan A, Aiello G, Féchant M, Aprili M, Gabelli J and Estève J 2018 *Phys. Rev. Lett.* **121** 043602
[72] Liu Z H and Xu X W 2024 *Phys. Rev. A* **110** 063705
[73] Born M and Wolf E 2019 *Principles of Optics: 60th Anniversary Edition* 7th ed (Cambridge University Press)
[74] Terrel M, Digonnet M J F and Fan S 2009 *Appl. Opt.* **48** 4874
[75] Khial P P, White A D and Hajimiri A 2018 *Nat. Photon.* **12** 671
[76] Zhao Y, Zhao H, Lv R Q and Zhao J 2019 *Opt. Lasers Eng.* **117** 7
[77] Chow W W, Gea-Banacloche J, Pedrotti L M, Sanders V E, Schleich W and Scully M O 1985 *Rev. Mod. Phys.* **57** 61
[78] Stedman G E 1997 *Rep. Prog. Phys.* **60** 615
[79] Li R, Fan W, Jiang L, Duan L, Quan W and Fang J 2016 *Phys. Rev. A* **94** 032109
[80] Ren J, Hodaei H, Harari G, Hassan A U, Chow W, Soltani M, Christodoulides D and Khajavikhan M 2017 *Opt. Lett.* **42** 1556
[81] Li J, Suh M G and Vahala K 2017 *Optica* **4** 346
[82] Sunada S 2017 *Phys. Rev. A* **96** 033842
[83] Li K, Davuluri S and Li Y 2018 *Sci. China Phys. Mech. Astron.* **61** 90311
[84] Carlo M D, Leonardis F D, Lamberti L and Passaro V M N 2019 *Opt. Lett.* **44** 3956
[85] Lai Y H, Lu Y K, Suh M G, Yuan Z and Vahala K 2019 *Nature* **576** 65
[86] Hokmabadi M P, Schumer A, Christodoulides D N and Khajavikhan M 2019 *Nature* **576** 70
[87] Mao X, Qin G Q, Yang H, Zhang H, Wang M and Long G L 2020 *New J. Phys.* **22** 093009
[88] Zhang H, Peng M, Xu X W and Jing H 2022 *Chin. Phys. B* **31** 014215
[89] Li K, Davuluri S and Li Y 2018 *Chin. Phys. B* **27** 084203
[90] Giazotto F, Heikkilä T T, Luukanen A, Savin A M and Pekola J P 2006 *Rev. Mod. Phys.* **78** 217
[91] Dedyulin S, Ahmed Z and Machin G 2022 *Meas. Sci. Technol.* **33** 092001
[92] Moreva E, Bernardi E, Traina P, Sosso A, Tchernij S D, Forneris J, Picollo F, Brida G, Pastuović Ž, Degiovanni I P, Olivero P and Genovese M 2020 *Phys. Rev. Appl.* **13** 054057
[93] Xu H, Hafezi M, Fan J, Taylor J M, Strouse G F and Ahmed Z 2014 *Opt. Express* **22** 3098
[94] Klimov N, Purdy T and Ahmed Z 2018 *Sensors and Actuators A: Physical* **269** 308
[95] Liao J and Yang L 2021 *Light Sci. Appl.* **10** 32
[96] Dong C H, He L, Xiao Y F, Gaddam V R, Ozdemir S K, Han Z F, Guo G C and Yang L 2009 *Appl. Phys. Lett.* **94** 231119
[97] Li B B, Wang Q Y, Xiao Y F, Jiang X F, Li Y, Xiao L and Gong Q 2010 *Appl. Phys. Lett.* **96** 251109
[98] Wang Q, Zhang J Q, Ma P C, Yao C M and Feng M 2015 *Phys. Rev. A* **91** 063827
[99] Purdy T P, Yu P L, Kampel N S, Peterson R W, Cicak K, Simmonds R W and Regal C A 2015 *Phys. Rev. A* **92** 031802
[100] Purdy T P, Grutter K E, Srinivasan K and Taylor J M 2017 *Science* **356** 1265
[101] Chowdhury A, Vezio P, Bonaldi M, Borrielli A, Marino F, Morana B, Pandraud G, Pontin A, Prodi G A, Sarro P M, Serra E and Marin F 2019 *Quantum Sci. Technol.* **4** 024007
[102] Galinskiy I, Tsaturyan Y, Parniak M and Polzik E S 2020 *Optica* **7** 718
[103] Singh R and Purdy T P 2020 *Phys. Rev. Lett.* **125** 120603
[104] Potts C, Bittencourt V, Kusminskiy S V and Davis J 2020 *Phys. Rev. Applied* **13** 064001
[105] Gardiner C W and Collett M J 1985 *Phys. Rev. A* **31** 3761
[106] Carmichael H 1993 *An Open Systems Approach to Quantum Optics* (Springer-Verlag Berlin Heidelberg)
[107] Zielińska J A and Mitchell M W 2017 *Opt. Lett.* **42** 5298
[108] Culshaw B 2005 *Meas. Sci. Technol.* **17** R1
[109] Hunger D, Steinmetz T, Colombe Y, Deutsch C, Hänsch T W and Reichel J 2010 *New J. Phys.* **12** 065038
[110] Liu G, Zhou W, Gromyko D, Huang D, Dong Z, Liu R, Zhu J, Liu J, Qiu C W and Wu L 2025 *Appl. Phys. Rev.* **12** 011308
[111] Senellart P, Solomon G and White A 2017 *Nat. Nanotechnol.* **12** 1026
[112] Ding X, Guo Y P, Xu M C, Liu R Z, Zou G Y, Zhao J Y, Ge Z X, Zhang Q H, Liu H L, Wang L J, Chen M C, Wang H, He Y M, Huo Y H, Lu C Y and Pan J W 2025 *Nat. Photon.* **19** 387
[113] Liu S, Wang Y, Saleem Y, Li X, Liu H, Yang C A, Yang J, Ni H, Niu Z, Meng Y, Hu X, Yu Y, Wang X, Cygorek M and Liu J 2025 *Nature* **643** 1234
[114] Thompson J D, Zwickl B M, Jayich A M, Marquardt F, Girvin S M and Harris J G E 2008 *Nature* **452** 72
[115] Sankey J C, Yang C, Zwickl B M, Jayich A M and Harris J G E 2010 *Nat. Phys.* **6** 707
[116] Wilson D J, Regal C A, Papp S B and Kimble H J 2009 *Phys. Rev. Lett.* **103** 207204
[117] Karuza M, Molinelli C, Galassi M, Biancofiore C, Natali R, Tombesi P, Di Giuseppe G and Vitali D 2012 *New J. Phys.* **14** 095015
[118] Flowers-Jacobs N E, Hoch S W, Sankey J C, Kashkanova A, Jayich A M, Deutsch C, Reichel J and Harris J G E 2012 *Appl. Phys. Lett.* **101** 221109
[119] Rohse P, Butlewski J, Klein F, Wagner T, Friesen C, Schwarz A, Wiesendanger R, Sengstock K and Becker C 2020 *Rev. Sci. Instrum.* **91** 103102
[120] Ruelle T, Jaeger D, Fogliano F, Braakman F and Poggio M 2022 *Rev. Sci. Instrum.* **93** 095003
[121] Cavillon M, Dragic P D and Ballato J 2017 *Opt. Lett.* **42** 3650
[122] Gao H, Jiang Y, Cui Y, Zhang L, Jia J and Jiang L 2018 *J. Lightwave Technol.* **36** 5881